Artesunate inhibits growth and induces apoptosis in human osteosarcoma HOS cell line in vitro and in vivo

Qiang XU[1], Zhao-xu LI[1], Hui-qin PENG[2], Zheng-wang SUN[1], Rui-lin CHENG[1], Zhao-ming YE[1], Wei-xu LI[†‡1]

(*[1]Department of Orthopaedics, the Second Affiliated Hospital, School of Medicine, Zhejiang University, Hangzhou 310009, China*)

(*[2]Department of Medical Microbiology and Parasitology, School of Medicine, Zhejiang University, Hangzhou 310058, China*)

[†]E-mail: liweixu@163.com

Abstract: This paper aims to investigate the effects of artesunate (ART) on growth and apoptosis in human osteosarcoma HOS cell line in vitro and in vivo and to explore the possible underlying mechanisms. Cell viability was measured by 3-(4,5-dimethylthiazol-2-yl)-2,5-diphenyltetrazolium bromide (MTT) assay. The induction of apoptosis was detected by light and transmission electron microscopy and flow cytometry. Western blot analysis was used to investigate the related mechanisms. Nude mice were further employed to investigate the antitumour activity of ART in vivo. MTT assay results demonstrated that ART selectively inhibits the growth of HOS cells in a dose- and time-dependent manner. Based on the findings of light and transmission electron microscopy, Hoechst 33258 staining, and fluorescein isothiocyanate (FITC)-annexin V staining, the cytotoxicity of ART in HOS cells occurs through apoptosis. With ART treatment, cytosolic cytochrome *c* was increased, Bax expression was gradually upregulated, Bcl-2 expression was downregulated, and caspase-9 and caspase-3 were activated. Thus, the intrinsic apoptotic pathway may be involved in ART-induced apoptosis. Cell cycle analysis by flow cytometry indicated that ART may induce cell cycle arrest at G_2/M phase. In nude mice bearing HOS xenograft tumours, ART inhibited tumour growth and regulated the expressions of cleaved caspase-3 and survivin, in agreement with in vitro observations. ART has a selective antitumour activity against human osteosarcoma HOS cells, which may be related to its effects on induction of apoptosis via the intrinsic pathway. The results suggest that ART is a promising candidate for the treatment of osteosarcoma.

Key words: Artesunate, Human osteosarcoma HOS cells, Apoptosis, Cell cycle, Nude mice, Chemotherapy
doi:10.1631/jzus.B1000373   **Document code:** A   **CLC number:** R96

1 Introduction

Osteosarcoma is the most common primary malignant tumour of the bone and occurs mainly in children and adolescents. The primary treatment is a combination of surgery and neoadjuvant chemotherapy. In localized osteosarcoma patients, the five-year survival rates are approximately 65%–75% (Mirabello *et al.*, 2009). However, the prognosis for patients with recurrence and metastases is quite poor (Fagioli *et al.*, 2008). Additionally, most of the neoadjuvant chemotherapy drugs have extensive side effects, and multidrug resistant cases are common, particularly with cisplatin and doxorubicin (Longhi *et al.*, 2000; Chou and Gorlick, 2006; Schwartz *et al.*, 2007). Over the past 35 years, there has been no significant improvement in chemotherapy for osteosarcoma (Jaffe, 2010). Hence, there is an urgent need for new chemotherapy agents which are more effective and safer.

Artesunate (ART) is a partially-synthetic derivative of artemisinin, which is extracted from the Chinese herb *Artemisia annua*, and has been approved by the Chinese government for the treatment of malaria. During its many years of use, ART has been well tolerated by patients, with little toxicity and no obvious side effects (Doherty *et al.*, 1999; Weerasinghe *et al.*, 2002; Adjuik *et al.*, 2004; Efferth

and Kaina, 2010). The therapeutic doses of ART for patients are about 2–10 mg/(kg·d) (Taylor *et al.*, 2006). Recently, it has been reported that ART also exerts potent antitumour activity towards a variety of human cancer cells in culture, as well as in certain animal models (Efferth *et al.*, 2001; 2007; Li L.N. *et al.*, 2007; Li S. *et al.*, 2009; Du *et al.*, 2010; Michaelis *et al.*, 2010). In addition, Berger *et al.* (2005) first reported that long-term treatment with ART in combination with standard chemotherapy prolonged the survival time of two cancer patients suffering from metastatic uveal melanoma. Possible mechanisms for the antitumour activity of ART include induction of tumour cell apoptosis or oncosis (Efferth *et al.*, 2007; Li *et al.*, 2009; Du *et al.*, 2010), inhibition of angiogenesis and downregulation of vascular endothelial growth factor expression (Dell′Eva *et al.*, 2004; Zhou *et al.*, 2007), induction of DNA damage (Li *et al.*, 2008), suppression of the hyperactive Wnt/β-catenin pathway (Li *et al.*, 2007), and inhibition of tumour invasion and metastasis (Rasheed *et al.*, 2010). Apart from these, Efferth *et al.* (2003) reported that oxidative stress, which seems to be necessary for the antimalarial effects of ART, also plays an important role in ART antitumour activity.

Little is known about the effects of ART on human osteosarcoma cells. In the present study, we evaluated the anti-proliferative activity of ART in osteosarcoma HOS cell line in vitro and in vivo. We also investigated the possible underlying mechanisms mediating the antitumour effects of ART in this cell line.

2 Materials and methods

2.1 Cell culture

Human osteosarcoma cell line HOS and human osteoblast cell line hFOB1.19 were both obtained from the Cell Collection of Chinese Academy of Sciences (Shanghai, China). HOS cells were cultured in Dulbecco's modified Eagle medium (DMEM) at 37 °C, while hFOB1.19 cells were grown in DMEM/F12 in the presence of 0.3 mg/ml G418 at 33.5 °C (Brama *et al.*, 2007). All cell cultures were supplemented with 10% (v/v) fetal bovine serum (GIBCO, Carlsbad, CA, USA), 100 U/ml penicillin, and 100 μg/ml streptomycin, and maintained in a humidified atmosphere of 5% (v/v) CO_2.

2.2 Chemicals and reagents

Solutions of ART (Guilin Pharmaceutical Co., Ltd., Guangxi, China) were freshly prepared in 0.05 g/ml sodium bicarbonate and diluted in cell culture media to the indicated final concentrations. Control groups contained sodium bicarbonate at a dilution (v/v) equivalent to that used for the highest concentration of ART-treated groups in vitro. Cisplatin (CDDP), Hoechst 33258, dimethyl sulfoxide (DMSO), and 3-(4,5-dimethylthiazol-2-yl)-2,5-diphenyltetrazolium bromide (MTT) were purchased from Sigma Chemical Co. (St. Louis, MO, USA). An annexin V/propidium iodide (PI) double-staining kit was obtained from BioVision Inc. (Mountain View, CA, USA). Anti-Bax and anti-Bcl-2 antibodies, as well as horseradish peroxidase (HRP)-conjugated goat anti-mouse and HRP-conjugated goat anti-rabbit secondary antibodies, were from Santa Cruz Biotechnology (CA, USA). Antibodies to caspase-3, caspase-9, cleaved caspase-3, cytochrome *c*, and survivin were from Cell Signaling Technologies (Danvers, MA, USA).

2.3 Cytotoxicity assay

To evaluate whether the inhibitory effect of ART on cell growth is general or selective, we used a normal cell line hFOB1.19 as a control. HOS and hFOB1.19 cells were seeded in 96-well plates at a density of 4000–6000 cells/well. After overnight incubation, the media were replaced with fresh media containing ART at 0, 10, 20, 40, 80, and 160 μmol/L, respectively, and the cells were cultured for 24, 48, or 72 h. Control wells received no ART. At each time point, 20 μl of MTT (5 mg/ml) solution was added to each well, and the plates were cultured at 37 °C for another 4 h. Then, the media were replaced with 150 μl of DMSO to dissolve the formazan crystals, and the absorbance (optical density) at 570 nm (OD_{570}) was measured with a microplate reader (Dynatech MR7000; Dynatech Laboratories, Inc., Chantilly, VA, USA). The rate of growth inhibition was calculated as: $IR=(1-OD_{570,test}/OD_{570,con})×100\%$, where IR is inhibition rate, $OD_{570,test}$ is OD_{570} of test well, and $OD_{570,con}$ is OD_{570} of control well.

2.4 Assessment of cell morphology

After ART exposure, cell morphology was examined by phase-contrast light microscopy (Olympus,

Tokyo, Japan). To confirm morphological changes of nuclei, HOS cells treated with or without 80 µmol/L ART for 48 h were collected, fixed in 4% (v/v) formaldehyde for 30 min, washed three times with phosphate buffer solution (PBS), stained with 10 µg/ml Hoechst 33258 for 15 min, and then examined under a fluorescence microscope (Olympus, Tokyo, Japan).

2.5 Electron microscopy

HOS cells were fixed with 2.5% (v/v) glutaraldehyde in 0.1 mol/L PBS (pH 7.4) for 2 h, washed with PBS, and post-fixed in 0.01 g/ml osmium tetroxide for 1 h. The cells were dehydrated in acetone and embedded in epoxy resin. Ultrathin sections were stained with uranyl acetate and lead citrate, and examined under a transmission electron microscope (Philips TECNAI10, FEI Company, Hillsboro, OR, USA).

2.6 Annexin V/PI assay

After 48 h of treatment with ART, floating and adherent HOS cells were collected, stained with PI and fluorescein isothiocyanate (FITC)-annexin V, and analyzed by FACSCalibur flow cytometer (BD Biosciences, San Jose, CA, USA). Early apoptotic cells were positive for annexin V and negative for PI, whereas late apoptotic cells undergoing secondary necrosis were positive for both annexin V and PI.

2.7 Western blot analysis

Treated with ART for 48 h, the cells were harvested, washed with ice-cold PBS, suspended in 200 µl of ice-cold solubilizing buffer (300 mmol/L NaCl, 50 mmol/L Tris-HCl (pH 7.6), 0.5% (v/v) Triton X-100, 2 mmol phenylmethanesulfonyl fluoride, 2 µl/ml aprotinin, and 2 µl/ml leupeptin), and incubated at 4 °C for 1 h. The extracts were cleared by centrifugation at 13000 r/min for 20 min at 4 °C, and the protein content was quantified using a bicinchoninic acid (BCA) protein assay kit (Pierce, Rockford, IL, USA) according to the manufacturer's instructions. Equivalent amounts of proteins were separated by 0.08–0.12 g/ml sodium dodecyl sulfate-polyacrylamide gel electrophoresis (SDS-PAGE) and transferred to polyvinylidene difluoride (PVDF) membranes. The blots were blocked with 0.05 g/ml non-fat dry milk, incubated with primary antibody overnight at 4 °C, and then incubated with HRP-conjugated secondary antibody for 1 h at room temperature. Immunoreactive proteins were detected by enhanced chemiluminescence (Amersham Biosciences, Piscataway, USA), followed by exposure to X-ray film.

2.8 Cell cycle analysis

HOS cells were cultured in 6-well plates overnight and then incubated with fresh medium containing 0, 20, 40, or 80 µmol/L ART for 48 h. Floating and adherent cells were collected, washed with PBS, and fixed with 70% (v/v) ice-cold methanol overnight at 4 °C. The fixed cells were collected by centrifugation, washed with PBS, and resuspended in 0.5 ml of PBS containing 40 µg/ml RNase A and 50 µg/ml PI. Then they were examined with a FACSCalibur flow cytometer.

2.9 Antitumour effect of ART in vivo

Female BALB/c-nu mice (4–6 weeks old) were purchased from Shanghai Laboratory Animal Center of Chinese Academy of Sciences. They were maintained under specific pathogen-free conditions and supplied with sterilized food and water. Tumours were established by subcutaneous injection of 5×10^6 HOS cells into the flank of each mouse. The length (l) and width (b) of the tumour along with the body weights of the mice were measured twice weekly. The volume (V) of each tumour was estimated according to the formula: $V=l\times b^2/2$. When the tumours reached a volume of around 120 mm^3 at about two weeks, the mice were randomly divided into five groups ($n=6$): negative control group (mice injected intraperitoneally with 100 µl of saline once daily), positive drug control group (mice injected intraperitoneally with 2 mg/kg cisplatin twice weekly), and three ART groups (mice injected intraperitoneally with 50, 100, or 200 mg/kg ART once daily). The mice were closely monitored, and after 18 d, all mice were anesthetized by ether and sacrificed by neck dissection. The tumours were removed, weighed, and fixed in formalin for further analysis. All treatment protocols were approved by the Animal Care and Use Committee of Zhejiang University, China.

2.10 Immunohistochemistry

For immunohistochemical analyses of cleaved

caspase-3 and survivin, formalin-fixed tumour specimens were embedded in paraffin and sectioned. The sections were autoclaved at 121 °C for 10 min in citric acid solution (pH 6.0) for antigen retrieval. After quenching of endogenous peroxidase activity and blocking of non-specific binding sites, the sections were incubated with primary antibodies against cleaved caspase-3 or survivin (diluted 1:300), overnight at 4 °C. After washed three times with PBS again, the sections were incubated in secondary antibody (biotinylated goat anti-rabbit IgG diluted 1:500) for 30 min at 37 °C, washed, and then incubated with streptavidin-peroxidase conjugate for 30 min at 37 °C. Immunoreactivity was visualized by incubation with 3′-diaminobenzidine (Sigma, USA) for 5 min. Hematoxylin was used for background counterstaining.

2.11 Statistical analysis

All quantitative assays were performed in triplicate. The results are expressed as mean±standard deviation (SD). Statistical analysis of the difference between treated and untreated groups was performed with Student's *t*-test. Values of $P<0.05$ were considered to indicate significant differences.

3 Results

3.1 Inhibition of proliferation of HOS cells in a dose- and time-dependent manner

We examined the effects of ART on the viabilities of HOS and hFOB1.19 cells using an MTT assay. As shown in Fig. 1a, ART markedly inhibited the growth of HOS cells in a dose- and time-dependent manner, while hFOB1.19 cells were more resistant to ART. The half maximal inhibitory concentration (IC_{50}) values of ART on HOS and hFOB1.19 cells at 48 h were 52.8 and 206.3 μmol/L, respectively. The data suggests that ART induces selective cytotoxicity in human osteosarcoma cells.

3.2 Induction of morphological changes of HOS cells

Untreated HOS cells grew well with clearly visible cytoskeletons, as seen by phase contrast microscopy. After 48 h of treatment, ART produced broken, necrosed, and detached cells in a dose-

dependent manner, which was consistent with the growth inhibition (Fig. 1b). ART-treated HOS cells stained with the fluorescent DNA-binding dye Hoechst 33258 displayed condensed and fragmented nuclei, which are typical morphological features of apoptotic cells. In contrast, no morphological signs of apoptosis were observed in untreated cells (Fig. 1c). Transmission electron microscopic observations of the ultrastructural features in HOS cells revealed intact nucleoli, homogeneous chromatin, and visible microvilli in control cells. In contrast, cells treated with 80 μmol/L ART showed condensed chromatin, an irregular nuclear membrane, and cytoplasmic vacuoles, with no detectable microvilli (Fig. 1d).

3.3 Induction of apoptosis in HOS cells

To further confirm the rates of ART-induced cellular apoptosis, HOS cells were treated with various concentrations of ART for 48 h, stained with annexin V/PI, and then analyzed by flow cytometry. As shown in Fig. 2, the percentage of early apoptotic cells (annexin V^+/PI^-) in the control group was 1.74%, whereas cells treated with 20, 40, and 80 μmol/L ART had early apoptotic rates of 13.77%, 27.89%, and 32.58%, respectively. The results suggest that ART induced apoptosis in HOS cells in a dose-dependent manner.

3.4 Apoptotic signalling pathways

To investigate the mechanism by which ART induces apoptosis, we analyzed the expressions of apoptotic proteins in HOS cells, using Western blots. As shown in Fig. 3, ART dose-dependently stimulated the protein levels of cytochrome *c*, Bax, cleaved caspase-3, and cleaved caspase-9, while decreasing the protein levels of pro-caspase-3, pro-caspase-9, Bcl-2, and survivin. Additionally, the ratio of Bax/Bcl-2 was elevated, which may contribute to the apoptotic process.

3.5 Induction of cell cycle distribution changes of HOS cells

The cell cycle distribution of HOS cells treated with ART for 48 h was analyzed by flow cytometry. Compared with control cells, cells treated with 20, 40, and 80 μmol/L ART had a decreased proportion of cells in G_0/G_1 phase and a significantly increased proportion of cells in G_2/M phase (Fig. 4).

3.6 Inhibition of growth of HOS solid tumours in vivo

On the basis of our in vitro results, we examined the effects of ART on the growth of HOS cells in mouse xenograft models. When the tumour volumes reached about 120 mm^3, the mice were sorted into five groups to begin treatment. After 18 d of treatment, the tumour volumes in ART-treated and CDDP-treated mice were reduced compared with the volume in negative control mice (Fig. 5a). Furthermore, ART dose-dependently inhibited tumour growth. At an ART concentration of 200 mg/kg, the maximum rate of inhibition was reached, and it was not significantly different from that in the CDDP-treated positive control group ($P>0.05$). The average body weight of mice in all treatment groups, including the negative control group, tended to decrease as the protocol continued, with CDDP treatment causing more severe body weight loss than ART treatment (Table 1). This suggests that nude mice are more tolerant of ART than CDDP.

Table 1 Average body weight of mice in every group

Groups	Body weight (g)	
	Beginning	End
Control (saline)	18.3±0.9	18.0±0.6
50 mg/kg ART	18.4±1.0	17.6±0.6
100 mg/kg ART	18.7±0.7	17.3±0.9
200 mg/kg ART	18.8±0.9	16.7±0.8[*]
CDDP	18.6±0.8	15.7±0.5[**]

[*] $P<0.05$, [**] $P<0.01$, compared with the control (saline) group
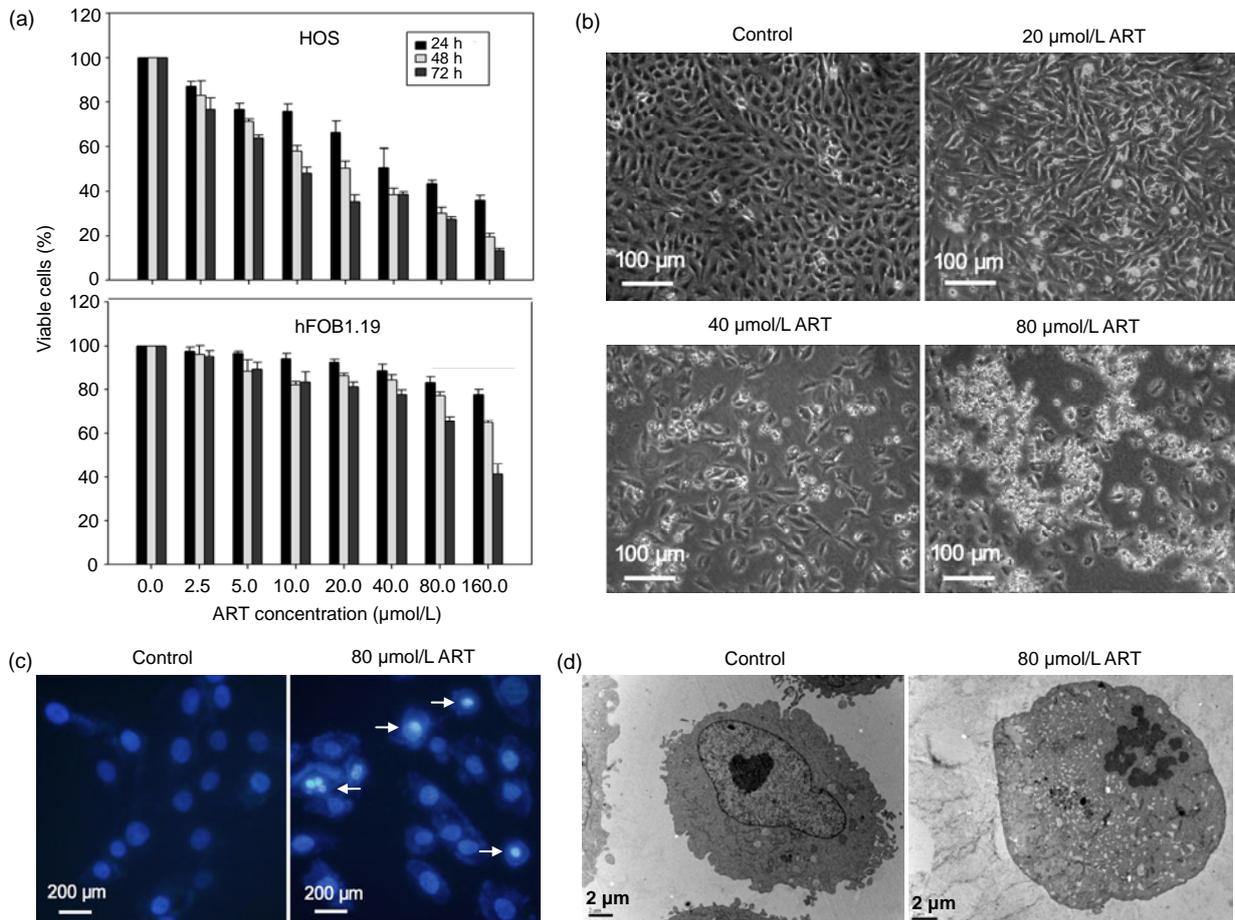
Fig. 1 Effects of ART on cell proliferation and morphological changes
(a) Human osteosarcoma HOS cells and human osteoblast hFOB1.19 cells were treated with various concentrations of ART for 24, 48, and 72 h, and the inhibition of cell growth was measured by MTT assay. Results are expressed as mean±SD of three independent experiments. (b) HOS cells were treated with 0, 20, 40, or 80 μmol/L ART for 48 h. Morphological changes were examined and photographed under a phase contrast microscope. (c) HOS cells were treated with or without 80 μmol/L ART for 48 h, stained with Hoechst 33258, and observed under a fluorescence microscope. (d) After treatment with or without 80 μmol/L ART for 48 h, HOS cells were examined for ultrastructural morphological features of apoptosis by transmission electron microscopy

(a)

(b)
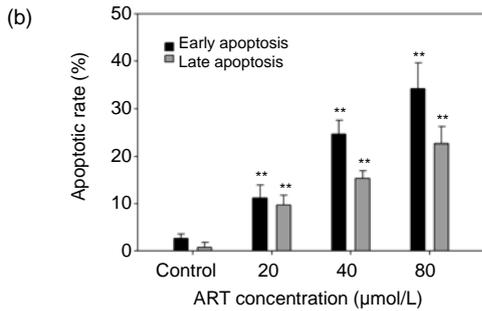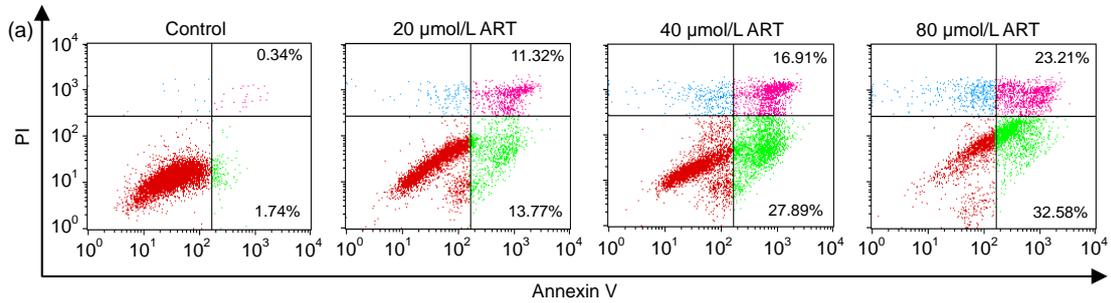
Fig. 2 Flow cytometric analysis of ART-induced apoptosis in HOS cells using FITC-annexin V/PI staining
(a) HOS cells were treated with 0, 20, 40, or 80 μmol/L ART for 48 h and stained with FITC-annexin V/PI. Apoptotic and necrotic cell populations were analyzed by flow cytometry. Cells in the lower right quadrant represent early apoptotic cells, and cells in the upper right quadrant represent late apoptotic cells undergoing secondary necrosis. Data are representative of three similar experiments. (b) The early and late apoptotic rates of HOS cells induced by ART. [**] $P<0.01$, compared with the control group
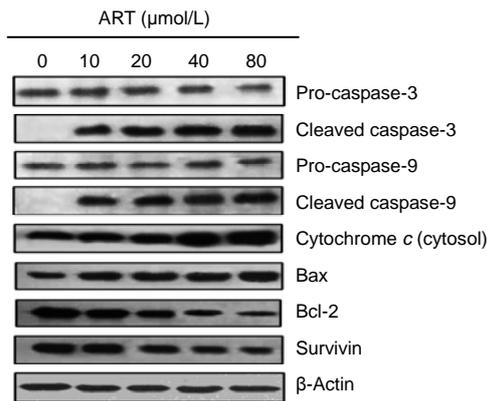
Fig. 3 Effects of ART on the expressions of apoptosis-related proteins
Following treatment of HOS cells with different concentrations of ART for 48 h, caspase-3, caspase-9, cytochrome c, Bax, Bcl-2, and survivin protein expression levels were analyzed by Western blots. Data are representative of three independent experiments

3.7 Immunohistochemical studies of xenograft tumour tissues

We evaluated the expressions of apoptosis-related proteins in tumour tissues by immunohisto-chemical staining of cleaved caspase-3 and survivin. Figs. 5b and 5c show representative staining of cleaved caspase-3 and survivin, respectively, in mouse tumour tissues. Compared to the negative control group, there was a marked increase in cleaved caspase-3 expression and a decrease in survivin expression in mice treated with 200 mg/kg ART.
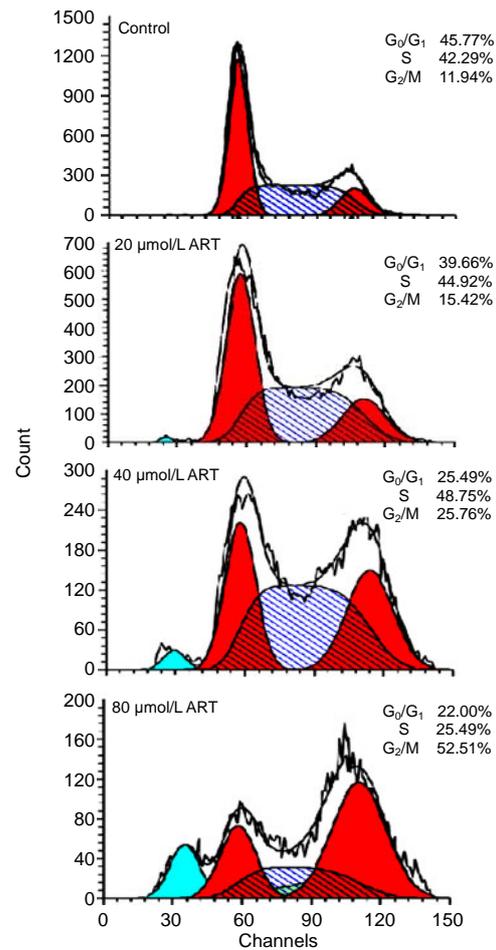

Fig. 4 Cell cycle analysis of HOS cells treated with ART
Cells were cultured with different concentrations of ART for 48 h and then stained with PI. Flow cytometry was used to analyze DNA at the G_1, S, and G_2 phases of the cell cycle. Data are representative of three similar experiments
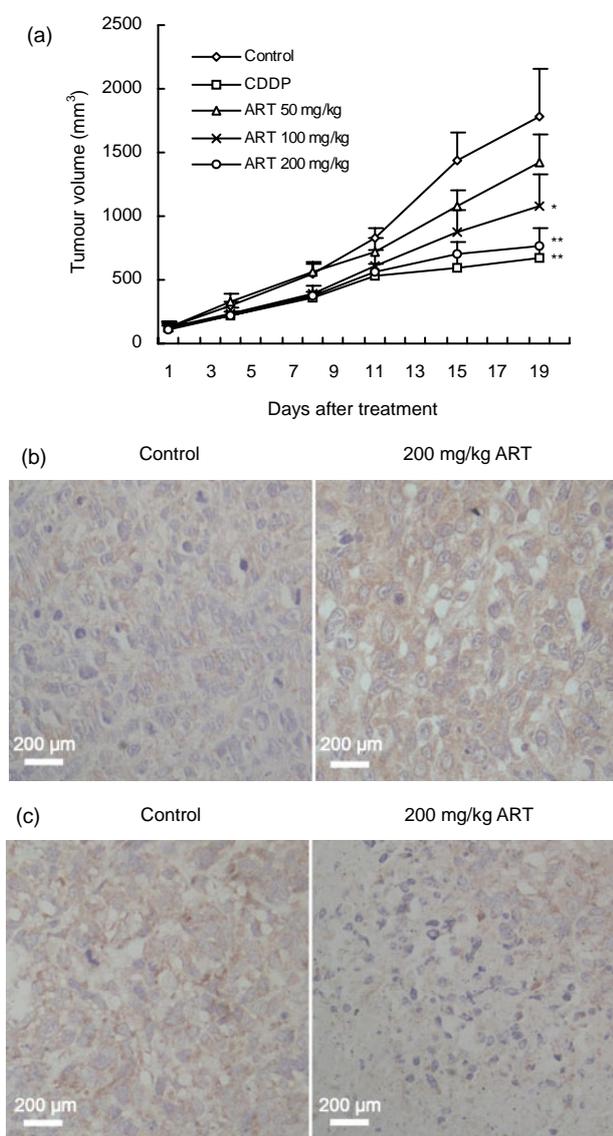
Fig. 5 Effects of ART on osteosarcoma HOS cell xenografts in vivo

(a) Tumour volume in nude mice treated with an i.p. injection of ART (50, 100, or 200 mg/kg) for 18 d. Saline and cisplatin (CDDP, 2 mg/kg) were used as negative and positive controls, respectively. * $P<0.05$, ** $P<0.01$, significant difference in tumour volume compared with the negative control. (b) Representative immunochemical staining using an antibody that reacts with the active cleaved form of caspase-3. Tumour tissues were prepared from the negative control group and ART (200 mg/kg)-treated group. More apoptotic cells were observed in sections of the tumour from the mice given ART. (c) Representative immunochemical staining using anti-survivin antibody on tumour tissues from the negative control group and ART (200 mg/kg)-treated group. Survivin was primarily expressed in the cytoplasm of osteosarcoma cells, with less expression in the ART-treated group

4 Discussion

Osteosarcoma is a highly malignant disease. Although neoadjuvant chemotherapy can be effective, drug resistance and side effects remain serious problems that reduce the quality of life for the patients. To improve the prognosis for osteosarcoma, it is necessary to develop new anticancer agents with tumour-selective cytotoxicity. ART, which is an approved treatment option for multidrug-resistant malaria therapy, has an excellent safety profile. However, its biological activity has not been completely elucidated. Recently, the antitumour activity of ART has been described (Efferth et al., 2001; 2007; Berger et al., 2005; Li L.N. et al., 2007; Li S. et al., 2009; Du et al., 2010; Michaelis et al., 2010). In the present work, we report for the first time that ART can exert potent cytotoxic effects on human osteosarcoma HOS cell line in vitro and in vivo. The cytotoxicity of ART was mediated by apoptosis, which was further supported by both morphological features and expressions of apoptosis-related proteins. For example, Hoechst 33258 staining and electron microscopy observations revealed that ART treatment produced condensed and fragmented nuclei, an irregular nuclear membrane, and deceased microvilli on the cells, all of which are typical of apoptosis.

Apoptosis, also known as programmed cell death, plays important roles in maintaining cell homeostasis, and dysfunction of apoptotic signalling may cause serious conditions such as cancer and autoimmune disease (Mahoney and Rosen, 2005). In recent decades, apoptosis has been the most studied mechanism of anticancer therapy. And many factors participate in this process. The Bax and Bcl-2 proteins are members of the Bcl-2 family, which consists of both pro-apoptotic and anti-apoptotic proteins that exert opposing effects on mitochondria (Walensky, 2006). Bax can promote the release of cytochrome c from mitochondria into the cytosol to enhance apoptosis, whereas Bcl-2 is a potent suppressor of apoptosis and can block the release of cytochrome c by preserving the integrity of the mitochondrial membranes (Yang et al., 1997; Eskes et al., 2000; Walensky, 2006). According to Efferth et al. (2003), tumour cells transfected with the Bcl-2 gene were more resistant to ART than control cells. In the present study, we observed that ART markedly increased

Bax expression and decreased Bcl-2 expression in HOS cells in a dose-dependent manner. An increased Bax/Bcl-2 ratio results in the release of cytochrome *c* and the activation of pro-caspase-9 (Bossy-Wetzel and Green, 1999). Active caspase-9 then cleaves and activates pro-caspase-3 to initiate a cascade of additional caspase activation, culminating in apoptosis. Thus, ART-induced apoptosis of HOS cells may be closely correlated with the intrinsic pathway, which is regulated mainly by Bcl-2, Bax, and cytochrome *c* (Garcia-Fuster *et al.*, 2008). And this mechanism was also observed in doxorubicin-resistant T leukemia cells by Efferth *et al.* (2007). However, Du *et al.* (2010) reported that ART also could induce oncosis-like cell death in Panc-1 pancreatic cancer cells. Therefore, ART may act through distinct mechanisms of cytotoxicity in different cancer cell lines.

Survivin, a member of the inhibitor of apoptosis protein family (Altieri, 2003), is abundantly expressed in cancer cells, but minimally expressed in normal differentiated adult tissues. It participates in the control of apoptosis and the regulation of cell division. Survivin has been reported to mediate mitotic progression, with highest expression in the G_2/M phase (Uren *et al.*, 2000). Osaka *et al.* (2007) suggested that the expression level of survivin may be useful as an independent prognostic indicator for osteosarcoma patients. In the present study, survivin was strongly expressed in HOS cells, and its expression was decreased with ART treatment in a dose-dependent manner. Immunohistochemical staining of survivin gave a similar result in xenograft tumour tissues.

Many anticancer agents regulate the cell cycle in G_1, S, or G_2 phase. We tested whether ART could also inhibit cell cycle progression in osteosarcoma cells. In contrast to a study by Li *et al.* (2009), our results in HOS cells showed that ART arrested the cell cycle at G_2/M phase in a dose-dependent manner. The underlying mechanisms will be the focus of further investigation.

In this work, we also evaluated the short-middle term antitumour effects of ART by analyzing tumour volume in nude mice bearing HOS cells. The toxic effects of ART were analyzed by the loss of body weight. We gave mice the same doses of ART as the study by Li *et al.* (2009) and gained a similar result. For example, the mice were well tolerant and no deaths were recorded during the treatment periods. Additionally, ART also displayed superior antitumour activity against osteosarcoma in vivo.

In conclusion, the antitumour effects of ART on osteosarcoma cells in vitro and in vivo were investigated. ART inhibited the growth and induced apoptosis of HOS cells in a dose- and time-dependent manner and the intrinsic apoptotic pathway may be involved in the process. In addition, ART also dose-dependently induced G_2/M cell cycle arrest in HOS cells. These results suggest that ART is a promising candidate drug for the treatment of osteosarcoma, and further preclinical trials are warranted.

References

Adjuik, M., Babiker, A., Garner, P., Olliaro, P., Taylor, W., White, N., 2004. Artesunate combinations for treatment of malaria: meta-analysis. *Lancet*, **363**(9402):9-17. [doi: 10.1016/S0140-6736(03)15162-8]

Altieri, D.C., 2003. Survivin, versatile modulation of cell division and apoptosis in cancer. *Oncogene*, **22**(53): 8581-8589. [doi:10.1038/sj.onc.1207113]

Berger, T.G., Dieckmann, D., Efferth, T., Schultz, E.S., Funk, J.O., Baur, A., Schuler, G., 2005. Artesunate in the treatment of metastatic uveal melanoma—first experiences. *Oncol Reports*, **14**(6):1599-1603.

Bossy-Wetzel, E., Green, D.R., 1999. Caspases induce cytochrome *c* release from mitochondria by activating cytosolic factors. *J. Biol. Chem.*, **274**(25):17484-17490. [doi:10.1074/jbc.274.25.17484]

Brama, M., Rhodes, N., Hunt, J., Ricci, A., Teghil, R., Migliaccio, S., Rocca, C.D., Leccisotti, S., Lioi, A., Scandurra, M., *et al.*, 2007. Effect of titanium carbide coating on the osseointegration response in vitro and in vivo. *Biomaterials*, **28**(4):595-608. [doi:10.1016/j. biomaterials.2006.08.018]

Chou, A.J., Gorlick, R., 2006. Chemotherapy resistance in osteosarcoma: current challenges and future directions. *Expert Rev. Anticancer Ther.*, **6**(7):1075-1785. [doi:10. 1586/14737140.6.7.1075]

Dell′Eva, R., Pfeffer, U., Vene, R., Anfosso, L., Forlani, A., Albini, A., Efferth, T., 2004. Inhibition of angiogenesis in vivo and growth of Kaposi's sarcoma xenograft tumors by the anti-malarial artesunate. *Biochem. Pharmacol.*, **68**(12):2359-2366. [doi:10.1016/j.bcp.2004.08.021]

Doherty, J.F., Sadiq, A.D., Bayo, L., Alloueche, A., Olliaro, P., Milligan, P., von Seidlein, L., Pinder, M., 1999. A randomized safety and tolerability trial of artesunate plus sulfadoxine—pyrimethamine versus sulfadoxine-pyrimethamine alone for the treatment of uncomplicated malaria in Gambian children. *Trans. R. Soc. Trop. Med. Hyg.*, **93**(5):543-546. [doi:10.1016/S0035-9203(99)90376-0]

Du, J.H., Zhang, H.D., Ma, Z.J., Ji, K.M., 2010. Artesunate induces oncosis-like cell death in vitro and has antitumor

activity against pancreatic cancer xenografts in vivo. *Cancer Chemother. Pharmacol.*, **65**(5):895-902. [doi:10.1007/s00280-009-1095-5]

Efferth, T., Kaina, B., 2010. Toxicity of the antimalarial artemisinin and its dervatives. *Crit. Rev. Toxicol.*, **40**(5):405-421. [doi:10.3109/10408441003610571]

Efferth, T., Dunstan, H., Sauerbrey, A., Miyachi, H., Chitambar, C.R., 2001. The anti-malarial artesunate is also active against cancer. *Int. J. Oncol.*, **18**(4):767-773.

Efferth, T., Briehl, M.M., Tome, M.E., 2003. Role of antioxidant genes for the activity of artesunate against tumor cells. *Int. J. Oncol.*, **23**(4):1231-1235.

Efferth, T., Giaisi, M., Merling, A., Krammer, P.H., Li-Weber, M., 2007. Artesunate induces ROS-mediated apoptosis in doxorubicin-resistant T leukemia cells. *PLoS One*, **2**(8):e693. [doi:10.1371/journal.pone.0000693]

Eskes, R., Desagher, S., Antonsson, B., Martinou, J.C., 2000. Bid induces the oligomerization and insertion of Bax into the outer mitochondrial membrane. *Mol. Cell Biol.*, **20**(3):929-935. [doi:10.1128/MCB.20.3.929-935.2000]

Fagioli, F., Biasin, E., Mereuta, O.M., Muraro, M., Luksch, R., Ferrari, S., Aglietta, M., Madon, E., 2008. Poor prognosis osteosarcoma: new therapeutic approach. *Bone Marrow Transplant.*, **41**(Suppl. 2):S131-S134. [doi:10.1038/bmt.2008.71]

Garcia-Fuster, M.J., Ramos-Miguel, A., Rivero, G., La Harpe, R., Meana, J.J., Garcia-Sevilla, J.A., 2008. Regulation of the extrinsic and intrinsic apoptotic pathways in the prefrontal cortex of short- and long-term human opiate abusers. *Neuroscience*, **157**(1):105-119. [doi:10.1016/j.neuroscience.2008.09.002]

Jaffe, N., 2010. Osteosarcoma: review of the past, impact on the future. The American experience. *Cancer Treat. Res.*, **152**(Part 3):239-262. [doi:10.1007/978-1-4419-0284-9_12]

Li, L.N., Zhang, H.D., Yuan, S.J., Tian, Z.Y., Wang, L., Sun, Z.X., 2007. Artesunate attenuates the growth of human colorectal carcinoma and inhibits hyperactive Wnt/β-catenin pathway. *Int. J. Cancer*, **121**(6):1360-1365. [doi:10.1002/ijc.22804]

Li, P.C., Lam, E., Roos, W.P., Zdzienicka, M.Z., Kaina, B., Efferth, T., 2008. Artesunate derived from traditional Chinese medicine induces DNA damage and repair. *Cancer Res.*, **68**(11):4347-4351. [doi:10.1158/0008-5472.CAN-07-2970]

Li, S., Xue, F., Cheng, Z., Yang, X., Wang, S., Geng, F., Pan, L., 2009. Effect of artesunate on inhibiting proliferation and inducing apoptosis of SP2/0 myeloma cells through affecting NFkappaB p65. *Int. J. Hematol.*, **90**(4):513-521. [doi:10.1007/s12185-009-0409-z]

Longhi, A., Porcu, E., Petracchi, S., Versari, M., Conticini, L., Bacci, G., 2000. Reproductive functions in female patients treated with adjuvant and neoadjuvant chemotherapy for localized osteosarcoma of the extremity. *Cancer*, **89**(9):1961-1965. [doi:10.1002/1097-0142(20001101)89:9<1961::AID-CNCR12>3.3.CO;2-#]

Mahoney, J.A., Rosen, A., 2005. Apoptosis and autoimmunity. *Curr. Opin. Immunol.*, **17**(6):583-588. [doi:10.1016/j.coi.2005.09.018]

Michaelis, M., Kleinschmidt, M.C., Barth, S., Rothweiler, F., Geiler, J., Breitling, R., Mayer, B., Deubzer, H., Witt, O., Kreuter, J., *et al.*, 2010. Anti-cancer effects of artesunate in a panel of chemoresistant neuroblastoma cell lines. *Biochem. Pharmacol.*, **79**(2):130-136. [doi:10.1016/j.bcp.2009.08.013]

Mirabello, L., Troisi, R.J., Savage, S.A., 2009. Osteosarcoma incidence and survival rates from 1973 to 2004: data from the Surveillance, Epidemiology, and End Results Program. *Cancer*, **115**(7):1531-1543. [doi:10.1002/cncr.24121]

Osaka, E., Suzuki, T., Osaka, S., Yoshida, Y., Sugita, H., Asami, S., Tabata, K., Sugitani, M., Nemoto, N., Ryu, J., 2007. Survivin expression levels as independent predictors of survival for osteosarcoma patients. *J. Orthop. Res.*, **25**(1):116-121. [doi:10.1002/jor.20291]

Rasheed, S.A., Efferth, T., Asangani, I.A., Allgayer, H., 2010. First evidence that the anti-malarial drug artesunate inhibits invasion and in vivo metastasis in lung cancer by targeting essential extracellular proteases. *Int. J. Cancer*, **127**(6):1475-1485. [doi:10.1002/ijc.25315]

Schwartz, C.L., Gorlick, R., Teot, L., Krailo, M., Chen, Z., Goorin, A., Grier, H.E., Bernstein, M.L., Meyers, P., 2007. Multiple drug resistance in osteogenic sarcoma: INT0133 from the Children's Oncology Group. *J. Clin. Oncol.*, **25**(15):2057-2062. [doi:10.1200/JCO.2006.07.7776]

Taylor, W.R., Terlouw, D.J., Olliaro, P.L., White, N.J., Brasseur, P., ter Kuile, F.O., 2006. Use of weight-for-age-data to optimize tablet strength and dosing regimens for a new fixed-dose artesunate-amodiaquine combination for treating falciparum malaria. *Bull. World Health Organ.*, **84**(12):956-964. [doi:10.2471/BLT.06.031492]

Uren, A.G., Wong, L., Pakusch, M., Fowler, K.J., Burrows, F.J., Vaux, D.L., Choo, K.H., 2000. Survivin and the inner centromere protein INCENP show similar cell-cycle localization and gene knockout phenotype. *Curr. Biol.*, **10**(21):1319-1328. [doi:10.1016/S0960-9822(00)00769-7]

Walensky, L.D., 2006. BCL-2 in the crosshairs: tipping the balance of life and death. *Cell Death Differ.*, **13**(8):1339-1350. [doi:10.1038/sj.cdd.4401992]

Weerasinghe, K.L., Galappaththy, G., Fernando, W.P., Wickremasinghe, D.R., Faizal, H.M., Wickremasinghe, A.R., 2002. A safety and efficacy trial of artesunate, sulphadoxine-pyrimethamine and primaquine in *P. falciparum* malaria. *Ceylon Med. J.*, **47**(3):83-85.

Yang, J., Liu, X., Bhalla, K., Kim, C.N., Ibrado, A.M., Cai, J., Peng, T.I., Jones, D.P., Wang, X., 1997. Prevention of apoptosis by Bcl-2: release of cytochrome *c* from mitochondria blocked. *Science*, **275**(5303):1129-1132. [doi:10.1126/science.275.5303.1129]

Zhou, H.J., Wang, W.Q., Wu, G.D., Lee, J., Li, A., 2007. Artesunate inhibits angiogenesis and downregulates vascular endothelial growth factor expression in chronic myeloid leukemia K562 cells. *Vascul. Pharmacol.*, **47**(2-3):131-138. [doi:10.1016/j.vph.2007.05.002]